

## ARTICLE OPEN



# Mucosal delivery of a multistage subunit vaccine promotes development of lung-resident memory T cells and affords interleukin-17-dependent protection against pulmonary tuberculosis

Claudio Counoupas<sup>1,2</sup>, Kia C. Ferrell<sup>1,2</sup>, Anneliese Ashhurst<sup>1</sup>, Nayan D. Bhattacharyya<sup>1,2</sup>, Gayathri Nagalingam<sup>1</sup>, Erica L. Stewart<sup>1,2,3</sup>, Carl G. Feng<sup>1,2</sup>, Nikolai Petrovsky<sup>3</sup>, Warwick J. Britton<sup>1,2,4</sup> and James A. Triccas<sup>1,2,5</sup>

The development of effective vaccines against bacterial lung infections requires the induction of protective, pathogen-specific immune responses without deleterious inflammation within the pulmonary environment. Here, we made use of a polysaccharide-adjuvanted vaccine approach to elicit resident pulmonary T cells to protect against aerosol *Mycobacterium tuberculosis* infection. Intratracheal administration of the multistage fusion protein CysVac2 and the delta-inulin adjuvant Advax™ (formulated with a TLR9 agonist) provided superior protection against aerosol *M. tuberculosis* infection in mice, compared to parenteral delivery. Surprisingly, removal of the TLR9 agonist did not impact vaccine protection despite a reduction in cytokine-secreting T cell subsets, particularly CD4<sup>+</sup>IFN-γ<sup>+</sup>IL-2<sup>+</sup>TNF<sup>+</sup> multifunctional T cells. CysVac2/Advax-mediated protection was associated with the induction of lung-resident, antigen-specific memory CD4<sup>+</sup> T cells that expressed IL-17 and RORγT, the master transcriptional regulator of Th17 differentiation. IL-17 was identified as a key mediator of vaccine efficacy, with blocking of IL-17 during *M. tuberculosis* challenge reducing phagocyte influx, suppressing priming of pathogen-specific CD4<sup>+</sup> T cells in local lymph nodes and ablating vaccine-induced protection. These findings suggest that tuberculosis vaccines such as CysVac2/Advax that are capable of eliciting Th17 lung-resident memory T cells are promising candidates for progression to human trials.

npj Vaccines (2020)5:105; <https://doi.org/10.1038/s41541-020-00255-7>

## INTRODUCTION

Tuberculosis (TB) remains a major cause of morbidity and mortality worldwide, with 10 million new cases and 1.5 million deaths per year<sup>1</sup>. *Mycobacterium bovis* bacillus Calmette–Guérin (BCG) is currently the only licensed vaccine against TB, however, its efficacy varies greatly, especially against the adult pulmonary form of the disease<sup>2</sup>. The 2015 WHO End TB Strategy identified the development of a more effective and easily administered vaccine for controlling TB and halting the global epidemic<sup>3</sup>. In recent decades, extensive research has resulted in many new TB vaccine candidates, 14 of which are currently in human vaccine trials and are reviewed in detail elsewhere<sup>4</sup>. Recently, a Phase IIb clinical trial of the fusion protein vaccine M72/AS01<sub>E</sub> showed protective efficacy of 50% in *M. tuberculosis*-infected adults after 3 years<sup>5,6</sup>. Although promising, vaccines with higher efficacy are considered necessary to reduce TB incidence to the targets outlined in the End TB Strategy objectives<sup>3</sup>.

One of the major limitations of current vaccination strategies is that the administration route may not be optimal for the induction of memory immune responses at the site of pathogen entry, i.e., the lung. Pulmonary vaccine delivery has been hindered by the fact that most adjuvants are either unable to induce sufficient mucosal immunity or are too toxic to be administered to the lung<sup>7</sup>. However, recent evidence supports the idea that mucosal

vaccination may provide superior protection against respiratory *M. tuberculosis* infection over parenteral vaccination. For example, lung-resident CD4<sup>+</sup> memory T cells (T<sub>RM</sub>) induced after pulmonary vaccination with a recombinant influenza virus expressing *M. tuberculosis* antigens provided protection in the lung in the absence of circulating memory cells<sup>8</sup>. T<sub>RM</sub> induction has also been proposed as the possible mechanism of protection in macaques that demonstrate sterilizing immunity after intravenous vaccination with BCG and subsequent *M. tuberculosis* infection<sup>9</sup>. When administered through the mucosal route, BCG induced better protection compared to the intradermal immunization, which was linked to lung T<sub>RM</sub> and Th17 polarization of the CD4<sup>+</sup> T cells<sup>10</sup>. Th17 responses have been associated with the influx of neutrophils with bactericidal activity<sup>11</sup> and increased CD4<sup>+</sup> T cell recruitment to the lung after *M. tuberculosis* infection<sup>12</sup>. Vaccines inducing high levels of pulmonary IL-17 have demonstrated efficacy against *M. tuberculosis* in different animal models<sup>13,14</sup> although balancing the protective and pathogenic roles of IL-17 in the lung is a critical consideration<sup>15</sup>.

In this study we sought to determine if the candidate TB vaccine, CysVac2/Advax<sup>16</sup>, is effective as a mucosal vaccine to protect against *M. tuberculosis*. CysVac2 is a fusion protein of two *M. tuberculosis* antigens; the immunodominant Ag85B and CysD, a component of the sulfur assimilation pathway that is over-expressed in chronic stages of infection<sup>17</sup>. Advax is a particulate

<sup>1</sup>Discipline of Infectious Diseases and Immunology, School of Medical Sciences, Faculty of Medicine and Health, The University of Sydney, Camperdown, NSW, Australia.

<sup>2</sup>Tuberculosis Research Program Centenary Institute, The University of Sydney, Camperdown, NSW, Australia. <sup>3</sup>Vaxine Pty Ltd, 11 Walkley Avenue, Warradale and Flinders University, Adelaide, Australia. <sup>4</sup>Department of Clinical Immunology, Royal Prince Alfred Hospital, Camperdown, NSW 2050, Australia. <sup>5</sup>Charles Perkins Centre and Marie Bashir Institute for Infectious Diseases and Biosecurity, The University of Sydney, Camperdown, NSW, Australia. ✉email: claudio.counoupas@sydney.edu.au; jamie.triccas@sydney.edu.au

polysaccharide adjuvant with a low inflammatory profile that has proven to be safe and a strong inducer of vaccine immunogenicity in humans, thus making it an ideal candidate for mucosal administration<sup>18,19</sup>. Advax was recently shown to provide safe and effective enhancement of influenza vaccine immunity when administered via the intrapulmonary route in different animal models<sup>20,21</sup>. Notably, it is currently been used in Phase I clinical trial as part of COVAX-19, a candidate vaccine for COVID-19 (NCT04453852).

We report here that intrapulmonary administration of CysVac2/Advax-induced greater protection in mice than parenterally administered vaccine, with the vaccine promoting the accumulation of antigen-specific, IL-17-secreting CD4<sup>+</sup> T<sub>RM</sub> in the lungs. Furthermore, IL-17 was essential for the protective efficacy afforded by the intrapulmonary CysVac2/Advax vaccine, thus defining a crucial role for this cytokine in vaccine-mediated control of TB.

## RESULTS

Pulmonary administration of CysVac2/Advax<sup>CpG</sup> provides superior protection against *M. tuberculosis* challenge than parenteral vaccination

Previous studies of intramuscular (i.m.) vaccination of mice with CysVac2/Advax<sup>CpG</sup> demonstrated substantially enhanced systemic CD4<sup>+</sup> T cell responses composed of multifunctional Th1 polarized cells, which correlated with protection against aerosol *M. tuberculosis* infection<sup>16</sup>. In this study, we evaluated if delivery to the lung by intratracheal (i.t.) instillation of this vaccine candidate could improve the level of protection induced by this vaccine. Mice were vaccinated by either the i.t. or i.m. routes with CysVac2/Advax<sup>CpG</sup> three times, 2 weeks apart (Fig. 1a). When the vaccine-specific T cell response was examined in the blood prior to *M. tuberculosis* challenge (following the gating strategy outlined in Supplementary Fig. 1), a higher level of circulating polyfunctional CD4<sup>+</sup> T cells expressing IFN- $\gamma$  was present after i.m. vaccination (Fig. 1b and Supplementary Fig 2a), with the most prominent phenotype identified as multi-cytokine-secreting CD44<sup>+</sup> CD4<sup>+</sup> T cells (Fig. 1c). After i.t. vaccination with CysVac2/Advax<sup>CpG</sup>, PBMC-derived CD4<sup>+</sup> T cells expressing either IL-2, TNF, or IL-17 were more prominent when compared to the i.m. route (Fig. 1b). Both vaccination regimens induced similar proportions of T-bet expression in circulating CD4<sup>+</sup> T cells, however, i.t. vaccination induced a higher proportion of cells expressing ROR $\gamma$ T (Fig. 1d).

The pattern of CD4<sup>+</sup> T cells immune responses pre-*M. tuberculosis* challenge was compared to that after *M. tuberculosis* infection. In i.m. vaccinated mice, the greatest frequency of CD4<sup>+</sup> T cells observed were those secreting IFN- $\gamma$  or TNF (Fig. 1e) and this was dominated by cells with polyfunctional Th1 responses (IFN- $\gamma$ <sup>+</sup>IL-2<sup>+</sup>TNF<sup>+</sup>, Fig. 1f). I.t. vaccination with CysVac2/Advax<sup>CpG</sup> resulted in a high frequency of CD4<sup>+</sup> T cells secreting either IL-17 or TNF (Fig. 1e) or both cytokines (Supplementary Fig 2b); these T cell subsets were not observed after i.m. vaccination (Fig. 1e and Supplementary Fig. 2). Further, the frequency of CD4<sup>+</sup> T cells expressing ROR $\gamma$ T was significantly enhanced after i.t. vaccination compared to unvaccinated or i.m. vaccinated mice (Fig. 1g). Therefore, i.t. the vaccination of mice with CysVac2/Advax<sup>CpG</sup> results in a Th17-polarized T cell response post-*M. tuberculosis* exposure, which was not observed after i.m. immunization.

Considering the differential pattern of immune responses induced by varying the route of administration of CysVac2/Advax<sup>CpG</sup>, we next determined if this had an impact on protective efficacy. I.t. vaccinated mice challenged with low dose aerosol *M. tuberculosis*, demonstrated significantly enhanced lung protection when compared to i.m.-vaccinated or unvaccinated mice (Fig. 1h). A similar result was observed in the spleen, suggesting that i.t. vaccination might improve protection against disseminated infection (Fig. 1i). Taken together, these results demonstrate that pulmonary

vaccination with CysVac2/Advax<sup>CpG</sup> induces superior protection compared to i.m. vaccination and this is associated with an enhanced generation of Th17 cells in the circulation and in the lung.

CpG is dispensable for protection generated by pulmonary vaccination with CysVac2/Advax

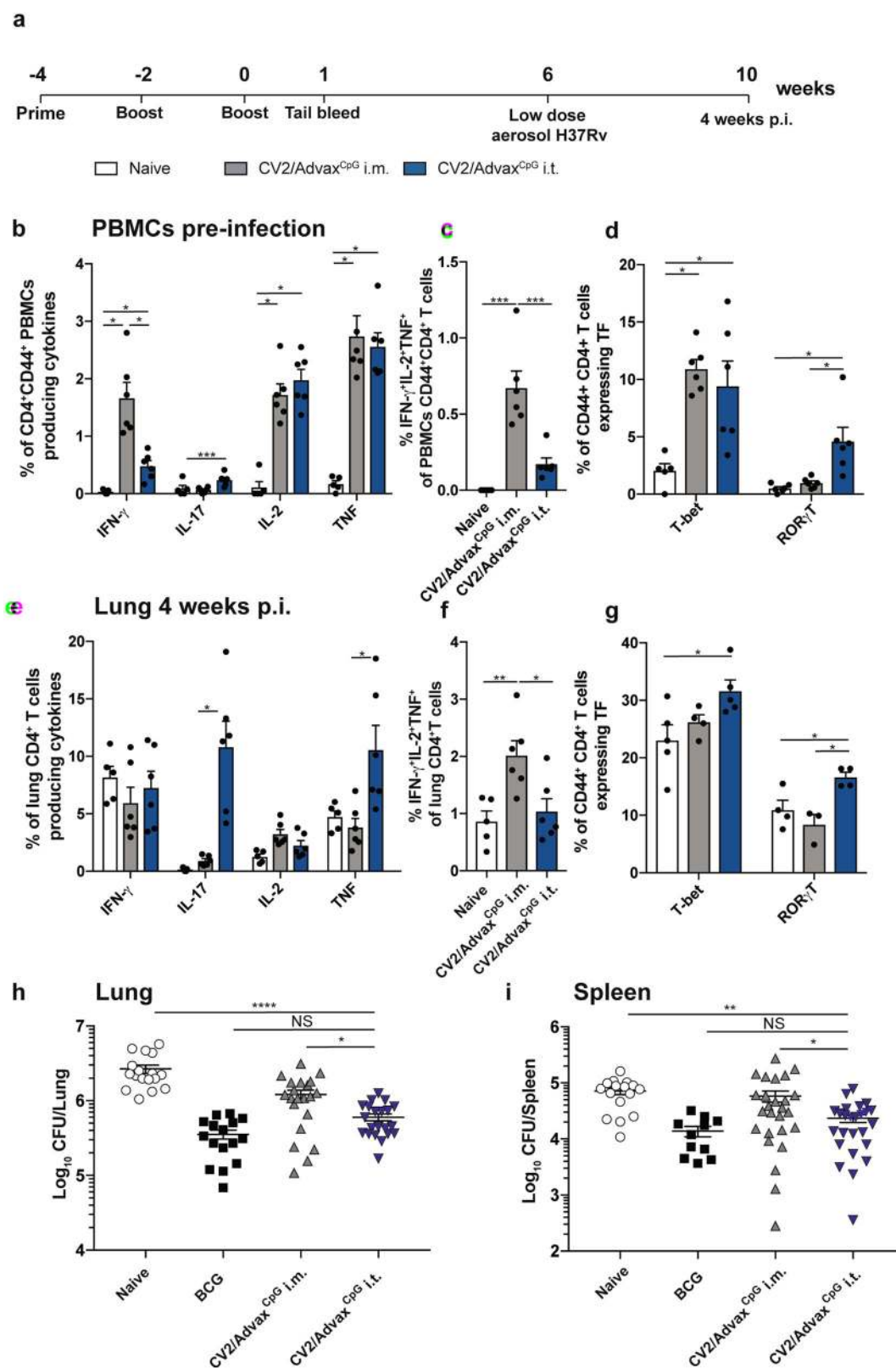
CpG oligonucleotides are TLR9 agonists that help drive Th1 immune responses<sup>22</sup>. While the CpG component was shown to be important to the protection obtained after CysVac2 i.m. immunization, we were interested whether a simplified formulation of Advax without the CpG component would still generate protective pulmonary immunity. CysVac2/Advax or CysVac2/Advax<sup>CpG</sup> were delivered by the i.t. route, and the mice challenged with aerosol *M. tuberculosis*. Both vaccines resulted in the generation of IL-17-producing CD4<sup>+</sup> T cells following antigen re-stimulation ex vivo (Fig. 2A), however, all inflammatory cytokines (IFN- $\gamma$ , IL-17, TNF) were reduced in Advax-immunized as compared to Advax<sup>CpG</sup>-vaccinated mice (Fig. 2a). Strikingly, the removal of the CpG component resulted in the loss of multifunctional CD4<sup>+</sup> T cells with a triple cytokine-secreting profile (IFN- $\gamma$ <sup>+</sup>IL-2<sup>+</sup>TNF<sup>+</sup>) (Fig. 2b and Supplementary Fig. 3). However, both vaccinated groups displayed equivalent expression of the transcription factors T-bet or ROR $\gamma$ T (Fig. 2c) and similar protection against *M. tuberculosis* in the lungs (Fig. 2c) and spleen (Fig. 2d). This indicates that CysVac2/Advax is sufficient for protection and this protection does not correlate with the presence of multifunctional T cells secreting high levels of inflammatory cytokines.

Intrapulmonary CysVac2/Advax stimulates antibody formation and iBalt formation in the lung

We further sought to define the immunogenic profile of CysVac2/Advax by defining the generation of humoral responses after pulmonary vaccination. Analysis of serum antibody titers revealed CysVac2-specific IgG1 antibodies at all time points examined, that was at least 1 log higher in the CysVac2/Advax group than mice vaccinated with antigen alone (Fig. 3a). IgG2c levels were comparatively lower than IgG1, particularly early after vaccination, but significantly greater at week 4 post-vaccination in CysVac2/Advax-vaccinated (Fig. 3b). We were also able to detect low levels of IgA in the serum of mice vaccinated i.t. with CysVac2/Advax, but not in other groups (Fig. 3c). Immunofluorescence staining of lung sections at 4 weeks post-infection identified the presence of agglomerates of T and B cells in peribronchial areas of the lung in mice vaccinated with CysVac2/Advax but not in mice vaccinated with PBS or CysVac2 alone, suggesting the formation of inducible Bronchial associated lymphoid tissue (iBalt) structures by the vaccine (Fig. 3d). Overall these observations indicate that mucosal vaccination with CysVac2/Advax is able to induce the secretion of CysVac2-specific antibodies and the formation of iBalt structures in the lung.

Intrapulmonary CysVac2/Advax generates lung-resident, antigen-specific CD4<sup>+</sup> T cells

To more precisely define the vaccine-specific cellular responses after immunization with CysVac2/Advax, Ag85B:I-A<sup>b</sup> tetramer staining was employed to identify CD4<sup>+</sup> T cells specific for the p25 epitope of Ag85B, an antigenic component of CysVac2<sup>17</sup>. Ag85B tetramer-positive (Ag85Btet<sup>+</sup>) cells in the lungs were only detected after i.t. delivery of CysVac2/Advax and not after CysVac2 antigen alone, confirming the critical role of Advax in inducing antigen-specific T cell expansion (Fig. 4a). Ag85Btet<sup>+</sup> cells were present in significantly greater numbers in CysVac2/Advax-vaccinated samples at all time points examined, although numbers contracted by 8 weeks post-vaccination (Fig. 4b). CysVac2/Advax-vaccinated mice showed enrichment of lung parenchymal-residing (intravascular negative IV<sup>-</sup>) CD4<sup>+</sup> T cells,



which expressed CD69 and CD44 with a low level of expression of the lymphoid homing receptor, L-selectin (CD62L) (Fig. 4d). This population of CD4<sup>+</sup>CD44<sup>hi</sup>CD62L<sup>low</sup>CD69<sup>+</sup> IV<sup>-</sup> were defined as T<sub>RM</sub>-like cells<sup>23</sup> and were significantly greater at all times points post-vaccination in CysVac2/Advax-vaccinated mice, comprising

approximately 25% of total CD4<sup>+</sup> T cells in the lung following vaccination (Fig. 4c). The majority of Ag85B-tet<sup>+</sup> cells detected at 8 weeks post-vaccination showed a T<sub>RM</sub>-like phenotype and were present within the parenchyma of the lung (Fig. 4e). Along with T<sub>RM</sub> markers, this subset expressed high levels of the integrin

**Fig. 1 Pulmonary vaccination with CysVac2/AdvaxCpG demonstrates improved protection against *M. tuberculosis* infection compared to parenteral administration.** C57BL/6 mice ( $n = 5-6$ ) were vaccinated by either the i.m. or i.t. route with CysVac2(CV2)/Advax<sup>CpG</sup> (three times, 2 weeks apart). One week after last vaccination mice were bled for vaccine immunogenicity assessment. Six weeks after last immunization mice were challenged with H37Rv by aerosol (~100 CFU) and 4 weeks later culled to enumerate the bacterial burden and the T cell phenotype in the lung (a). PBMCs from tail blood of vaccinated mice (b-d) or cells from lung of infected mice (e-g) were restimulated ex vivo with CysVac2, and the production of cytokines (IFN- $\gamma$ , IL-2, IL-17, TNF), or transcription factors (TF; T-bet, ROR $\gamma$ T) by CD4<sup>+</sup> T cells was determined by flow cytometry using the gating strategy described in Supplementary Fig. 1. Data are represented as the percentage of cytokine-producing or transcription factor-positive CD4<sup>+</sup> T cells  $\pm$  SEM. Bacterial load was assessed in the lungs (h) and in the spleen (i) and presented as log<sub>10</sub> of the mean CFU  $\pm$  SEM. Data are pooled from three independent experiments. The significance of differences between the groups was determined by ANOVA (\* $p < 0.05$ ; \*\* $p < 0.01$ ; \*\*\* $p < 0.001$ ).

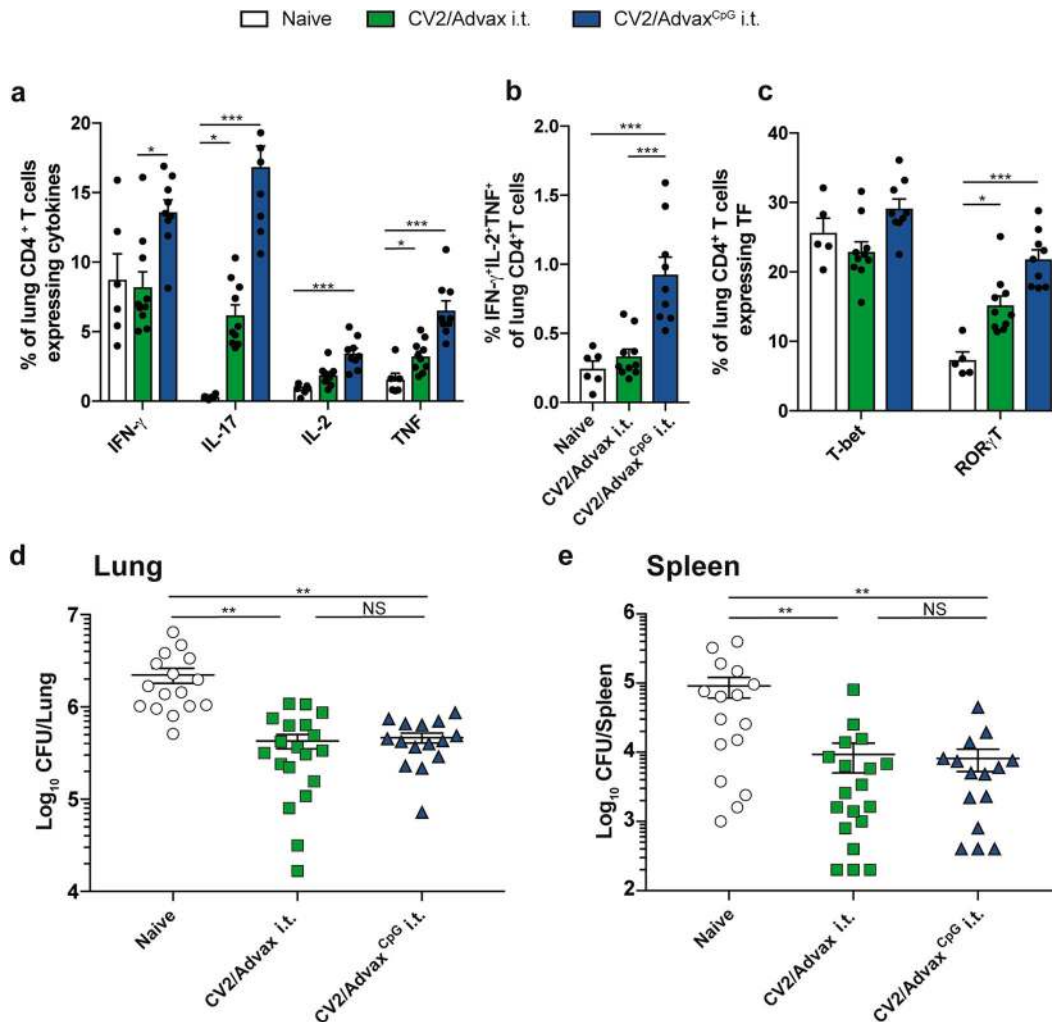


**Fig. 2 CpG is dispensable for protective immunity induced by CysVac2/Advax.** C57BL/6 mice ( $n = 5-10$ ) were vaccinated by the i.t. route with CysVac2/Advax<sup>CpG</sup> or CysVac2/Advax (three times, 2 weeks apart). Six weeks after last immunization mice were challenged with *M. tuberculosis* H37Rv by aerosol (~100 CFU) and four weeks later culled to enumerate the bacterial burden and the T cell phenotype in the lung. Cells from the lung of infected mice were restimulated ex vivo with CysVac2 and the production of cytokines (IFN- $\gamma$ , IL-2, IL-17, TNF (a, b)) or transcription factors (T-bet, ROR $\gamma$ T; (c)) by CD4<sup>+</sup> T cells was determined by flow cytometry using the gating strategy described in Supplementary Fig. 1. Data are represented as the percentage of cytokine-producing CD4<sup>+</sup> T cells  $\pm$  SEM. Bacterial load was assessed in the lungs (d) and in the spleen (e) and presented as log<sub>10</sub> of the mean CFU  $\pm$  SEM. Data are pooled from two independent experiments. The significance of differences between the groups was determined by ANOVA (\* $p < 0.05$ ; \*\* $p < 0.01$ ; \*\*\* $p < 0.001$ ).

CD11a and the cell surface receptor PD-1, with low levels of expression of CD103 and KLRG-1 (Fig. 4e). Taken together, these data indicate that CysVac2/Advax vaccination induces a population of antigen-specific CD4<sup>+</sup> T cells in the lung with a T<sub>RM</sub> phenotype, and these are detectable through 8 weeks post-vaccination.

We further characterized the ability of the CD4<sup>+</sup> T cells generated in the lung to produce cytokines in response to re-stimulation with

vaccine antigen at time points after vaccination (pre-challenge) as well as at 4 weeks post-challenge with *M. tuberculosis*. Intratracheal CysVac2/Advax vaccination induced a distinct cytokine profile that was relatively consistent across all time points prior to *M. tuberculosis* infection. While a marginal increase in IFN- $\gamma$  production was observed at 4 weeks post-vaccination, this was not apparent at any other time point (Fig. 4a). Indeed, following infection with *M. tuberculosis*, a lower percentage of IFN- $\gamma$ -producing CD4<sup>+</sup> T cells



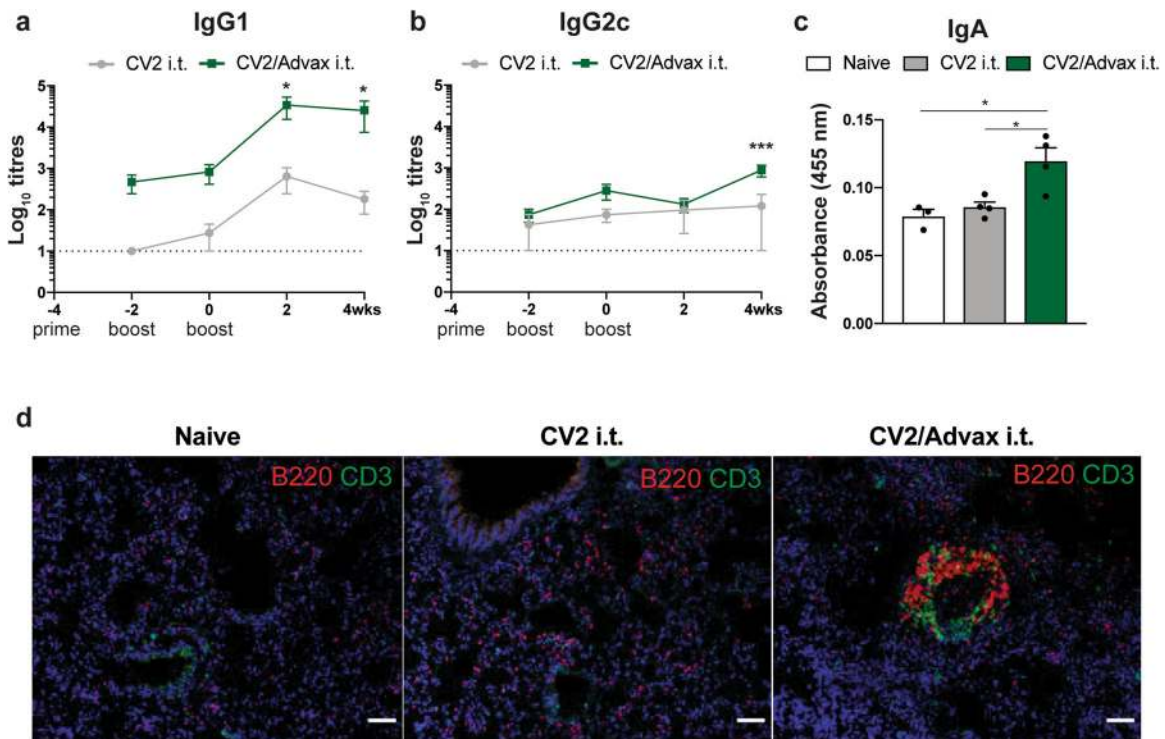


**Fig. 3 Pulmonary vaccination with CysVac2/Advax induces antigen-specific serum antibodies and the formation of iBALT in the lungs of vaccinated mice.** C57BL/6 mice ( $n = 3-4$ ) were vaccinated by the i.t. route with CysVac2/Advax or CysVac2 (three times, 2 weeks apart). Before the first and second boost, as well as 2 and 4 weeks after the second boost, mice were bled from the lateral tail vein and serum was collected. Titers of IgG1 (a) and IgG2c (b) were calculated by ELISA over the course of the time points examined. IgA (c) was measured by ELISA in the serum of week 2 samples. Data are represented as the average of  $\log_{10}$  titers  $\pm$  SEM or average 450 nm absorbance  $\pm$  SEM. Four weeks after the final vaccination, lung sections were stained with anti-mouse B220 (red) and anti-mouse CD3 (green) to visualize iBALT structures and imaged at  $\times 20$  magnification (d). Images are representative of three biological replicates/group; scale bars represent 50 microns. The significance of differences between the groups was determined by ANOVA ( $*p < 0.05$ ).

was present in CysVac2/Advax-vaccinated lung samples compared with samples from unvaccinated animals. By contrast, percentages of IL-2, IL-17, or TNF cytokine-producing cells were markedly increased after i.t. vaccination with CysVac2/Advax compared to unvaccinated or CysVac2 vaccinated mice up to 8 weeks post-vaccination (Fig. 5b–d), however only IL-17 remained elevated post-challenge (Fig. 5b). Further analysis revealed that the major source of IL-17 originated from CD45<sup>IV</sup>CD4<sup>+</sup> T cells that expressed ROR $\gamma$ T (Fig. 5e). Furthermore, the Ag85Btet<sup>+</sup> population was highly enriched in ROR $\gamma$ T<sup>+</sup> CD45<sup>IV</sup>IL-17<sup>+</sup>CD4<sup>+</sup> T cells (Fig. 5f). Overall, these data suggest that pulmonary vaccination with CysVac2/Advax promotes increased single and multifunctional cytokine-producing T cell populations both before and after aerosol challenge with *M. tuberculosis*, which is characterized by the development of a tissue-resident Th17-type response.

IL-17-mediated protection correlates with early recruitment of phagocytic cells and enhanced priming of pathogen-specific CD4<sup>+</sup> T cells

Given the marked Th17 polarization of the CD4<sup>+</sup> T cell response to pulmonary immunization with CysVac2/Advax, we next determined the impact of neutralizing IL-17 at the time of *M. tuberculosis* challenge (Fig. 6a). Treatment with anti-IL-17 mAb did not affect the capacity of CD4<sup>+</sup> T cells to respond to infection, as the frequency of cytokine-producing CD4<sup>+</sup> T cells was not altered between mice treated with anti-IL-17 or isotype control mAb (Fig. 6b). However, anti-IL-17 treatment had a detrimental effect on control of bacterial infection in the lung of CysVac2/Advax-immunized mice; bacteria numbers in anti-IL-17-treated mice were similar to unvaccinated mice, while immunized mice

treated with isotype control mAb remained protected against infection (Fig. 6c).

We also studied the impact of IL-17 blocking on lung cell subsets after *M. tuberculosis* infection using flow cytometry phenotyping combined with an unsupervised visual implementation of *t*-distributed stochastic neighbor embedding (tSNE) analysis. The generated tSNE plot was calculated with 12 parameters and 10 clusters obtained using unsupervised analysis were subsequently assigned to a specific cell population (Fig. 6d), according to the expression level of each marker and previously described phenotypes (Supplementary Fig. 4). This analysis revealed that the percentage of neutrophils in the lung were elevated in vaccinated mice treated with control mAb, however, they returned to the level of unvaccinated animals after treatment with the anti-IL-17 mAb (Fig. 6e). A similar pattern was observed for monocytes and monocyte-derived-macrophages, however, no differences were observed for other phagocytic populations in the lung, such as alveolar macrophages (Fig. 6e).

We next investigated the effect of blocking IL-17 on the priming and proliferation of CD4<sup>+</sup> T cells. To do this, we examined CD4<sup>+</sup> T cells primed by the vaccination (Ag85B-tet<sup>+</sup>) and compared to T cells responding specifically to *M. tuberculosis* (ESAT6-tet<sup>+</sup>). In the lung, we observed a greater proportion of Ag85B-tet<sup>+</sup> cells in vaccinated mice compared to unvaccinated mice, however, anti-IL-17 treatment did not significantly alter the numbers of proliferating CD4<sup>+</sup> T cells (Supplementary Fig. 5a–c) or the numbers of Ag85B-tet<sup>+</sup> or ESAT6-tet<sup>+</sup> cells (Supplementary Fig. 5d–f). However, in the mLN of vaccinated mice a distinct vaccine-induced population of proliferating CD4<sup>+</sup> T cells expressing ROR $\gamma$ T was distinguishable (Fig. 7a). IL-17 blocking resulted in reduced proliferation of total CD4<sup>+</sup> T cells in the mLN of vaccinated mice

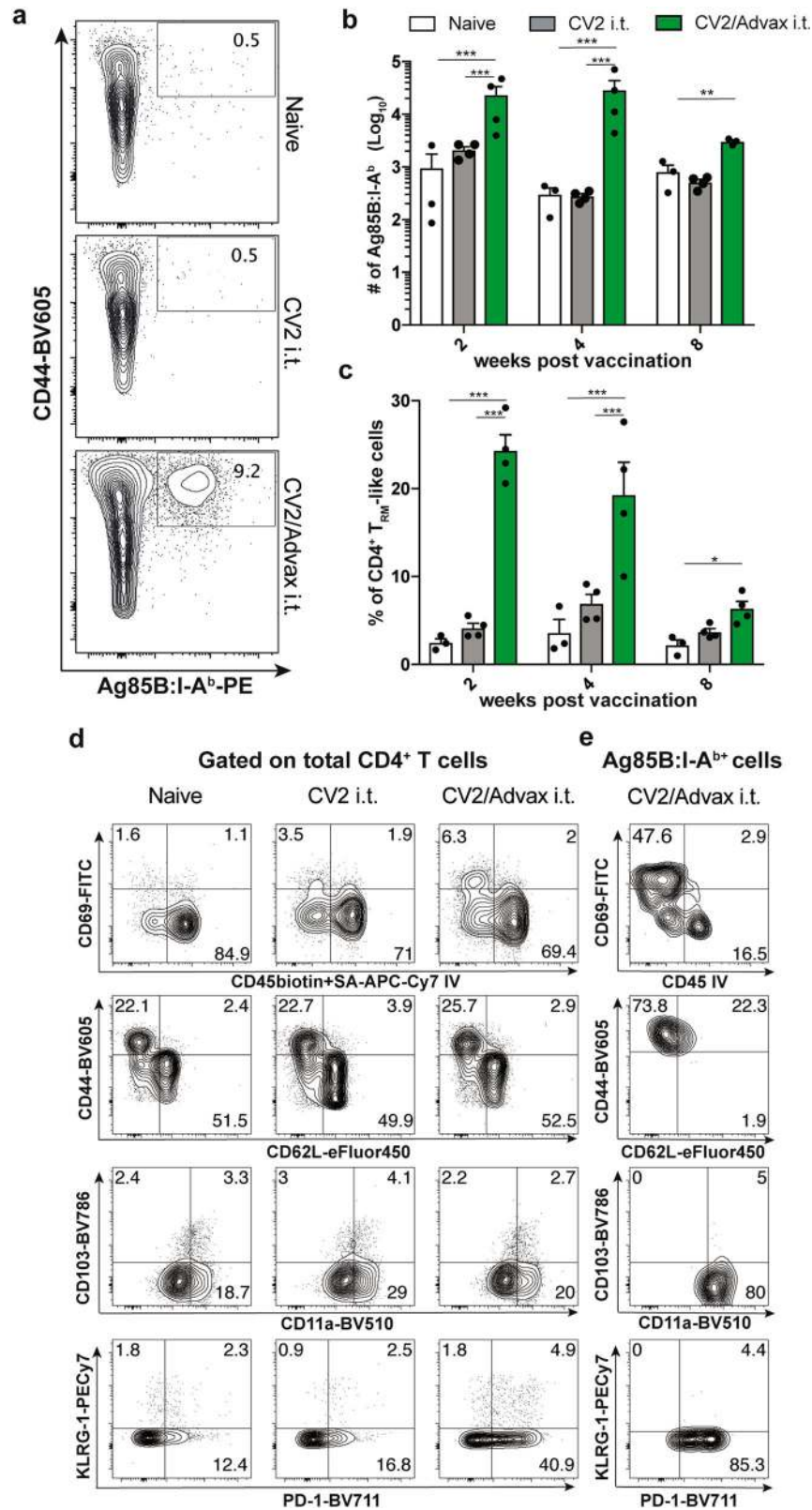


**Fig. 4 Pulmonary vaccination with CysVac2/Advax induces Ag-specific persistent local resident CD4<sup>+</sup> T cells.** C57BL/6 mice ( $n = 3-4$ ) were vaccinated by the i.t. route with CysVac2/Advax or CysVac2 (three times, 2 weeks apart). At weeks 2, 4, or 8 after the final immunization, lung cells were processed for Ag85B:I-A<sup>b</sup> tetramer staining. Representative dot plot from 8 weeks post-immunization of CD4<sup>+</sup> T cells gated as outlined in Supplementary Fig. 1 (a). Number of Ag85B:I-A<sup>b</sup> tetramer-positive cells in the lung over time are shown in b. Also shown are the percentage of total CD4<sup>+</sup> T cells expressing phenotypic markers associated with TRMs (CD45 IV<sup>-</sup>, CD11a<sup>+</sup>, CD69<sup>+</sup>, CD44<sup>+</sup>, PD-1<sup>+</sup> KLRG-1<sup>-</sup>) (c) and representative dot plots of TRM markers on total lung CD4<sup>+</sup> T cells (d) or in Ag85B:I-A<sup>b</sup>+ cells (e) at 8 weeks after last vaccination. Data are presented as mean  $\pm$  SEM and are representative of two independent experiments. The significance of differences between the groups was determined by ANOVA (\* $p < 0.05$ ; \*\* $p < 0.01$ ; \*\*\* $p < 0.001$ ).

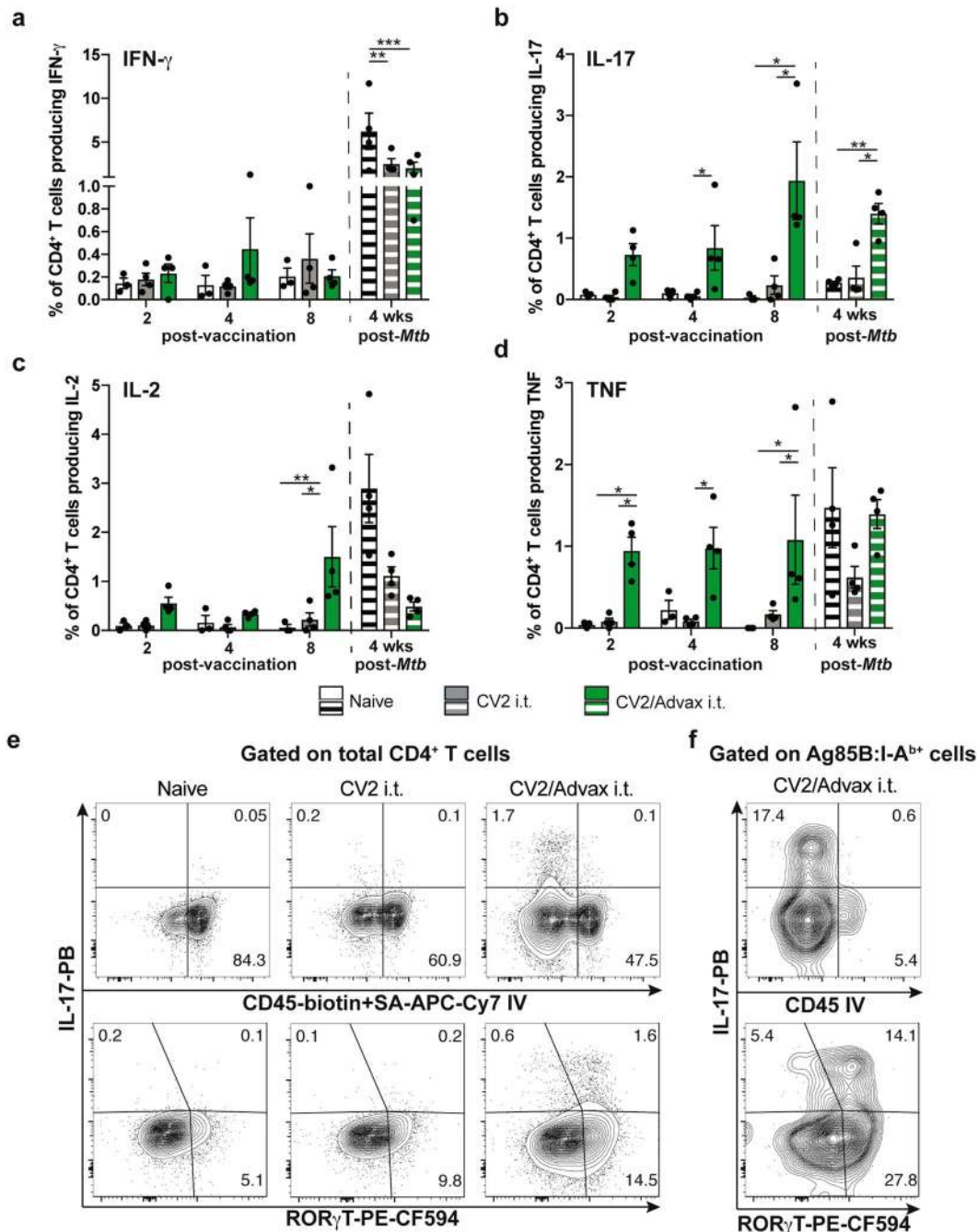


**Fig. 5** Persistent CysVac2-specific IL-17 production by lung-resident CD4<sup>+</sup> T cells after pulmonary vaccination with CysVac2/Advax. C57BL/6 mice ( $n = 3-5$ ) were vaccinated by the i.t. route with CysVac2/Advax or CysVac2 protein alone (three times, 2 weeks apart). Eight weeks after the last immunization mice were challenged with *M. tuberculosis* H37Rv by aerosol ( $\sim 100$  CFU). At 2, 4, or 8 weeks after last immunization (solid bars), and at 4 weeks after infection (striped bars), lung cells were restimulated ex vivo with CysVac2, and the production of IFN- $\gamma$  (**a**), IL-17 (**b**), IL-2 (**c**), or TNF (**d**) by CD4<sup>+</sup> T cells determined by flow cytometry using the gating strategy described in Supplementary Fig. 1. Representative dot plots of co-expression of CD45 IV or ROR $\gamma$ T with IL-17 by total CD4<sup>+</sup> T cells (**e**) or Ag85B:I-A<sup>b+</sup> tetramer-positive cells (**f**) at 8 weeks after last vaccination. Data are represented as the percentage of cytokine-producing CD4<sup>+</sup> T cells  $\pm$  SEM and are representative of two independent experiments. The significance of differences between the groups was determined by ANOVA ( $*p < 0.05$ ;  $**p < 0.01$ ;  $***p < 0.001$ ).

(Fig. 7b) including the vaccine-primed ROR $\gamma$ T<sup>+</sup> cells (Fig. 7c). When the frequency of the vaccine-primed CD4<sup>+</sup> T cells (Ag85B-tet<sup>+</sup>) was compared to those primed only by *M. tuberculosis* infection (ESAT6-tet<sup>+</sup>) (Fig. 7d), Ag85B-tet<sup>+</sup> cells were significantly higher in vaccinated mice compared to the unvaccinated group, however, anti-IL-17 treatment did not affect the numbers of Ag85B-tet<sup>+</sup>

cells (Fig. 7e). By contrast, the numbers of ESAT6-tet<sup>+</sup> positive CD4<sup>+</sup> T cells were reduced after IL-17 blocking in the mLNs (Fig. 7f). Overall, neutralizing IL-17 reduced phagocytic cells in the lung of immunized animals and the numbers of pathogen-specific CD4<sup>+</sup> T cells in the draining LNs, which correlated with a loss of vaccine-mediated protection.



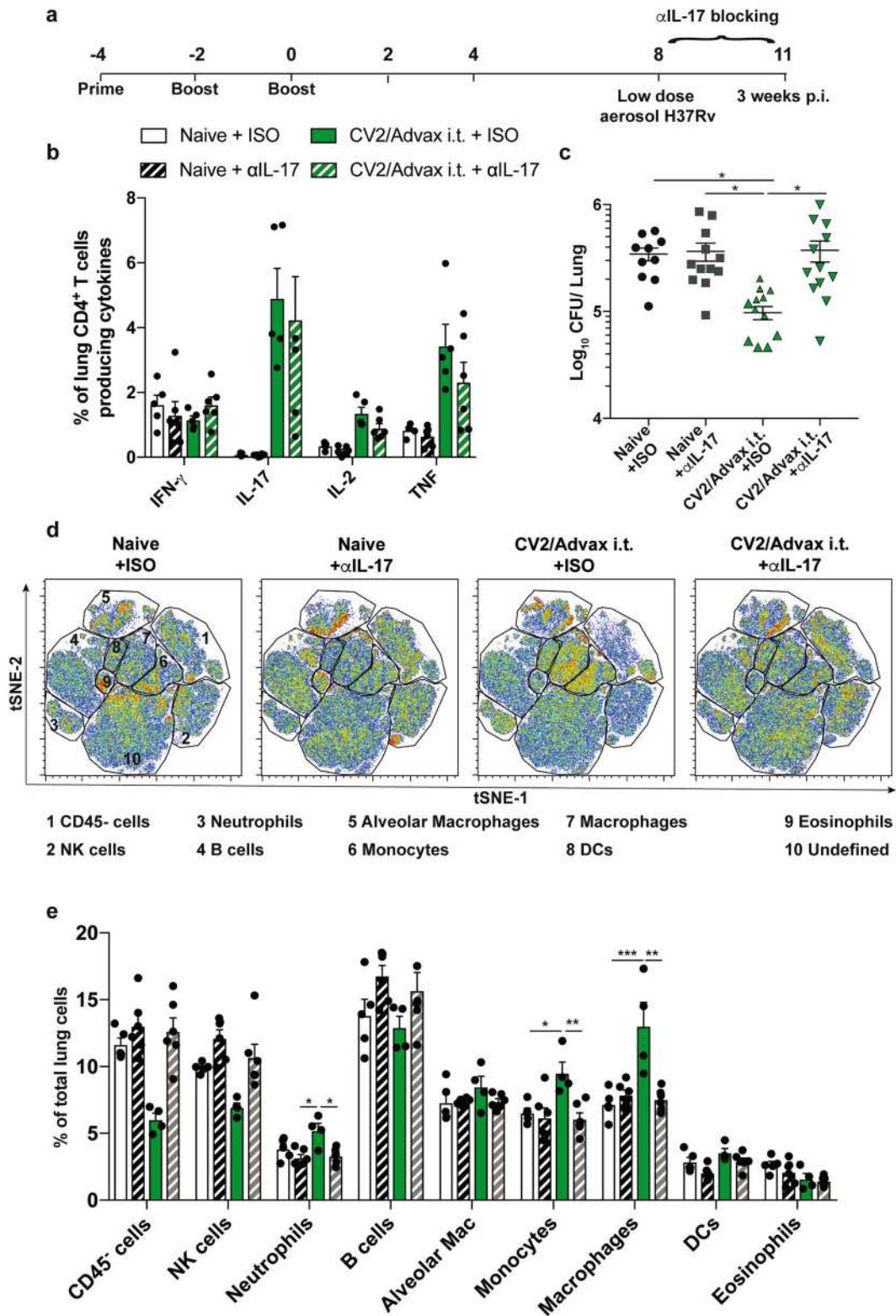


**Fig. 6 Protection afforded by pulmonary CysVac2/Advax against aerosol *M. tuberculosis* is dependent on IL-17 and correlates with lung phagocytic cell recruitment.** C57BL/6 mice ( $n = 5-6$ ) were vaccinated by the i.t. route with CysVac2/Advax (three times, 2 weeks apart), and at 8 weeks after the last immunization mice were challenged with *M. tuberculosis* H37Rv by aerosol (~100 CFU). One day before aerosol, mice were treated i.p. with anti-IL-17 or an isotype control mAb (twice weekly for 3 weeks) (a). Cells from the lungs of infected mice were restimulated ex vivo with CysVac2 and cytokines secretion (IFN- $\gamma$ , IL-2, IL-17, TNF) determined by flow cytometry using the gating strategy described in Supplementary Fig. 1 (b). Bacterial load was assessed in the lungs and is presented as Log<sub>10</sub> of the mean CFU  $\pm$  SEM (c). Representative tSNE dimensions 1 and 2 plots of the total live cells in the lung (d). Bar graphs show the average of the percentage  $\pm$  SEM of identified lung cell subsets (e). Data are pooled from two independent experiments. The significance of differences between the groups was determined by ANOVA (\* $p < 0.05$ ; \*\* $p < 0.01$ ; \*\*\* $p < 0.001$ ).



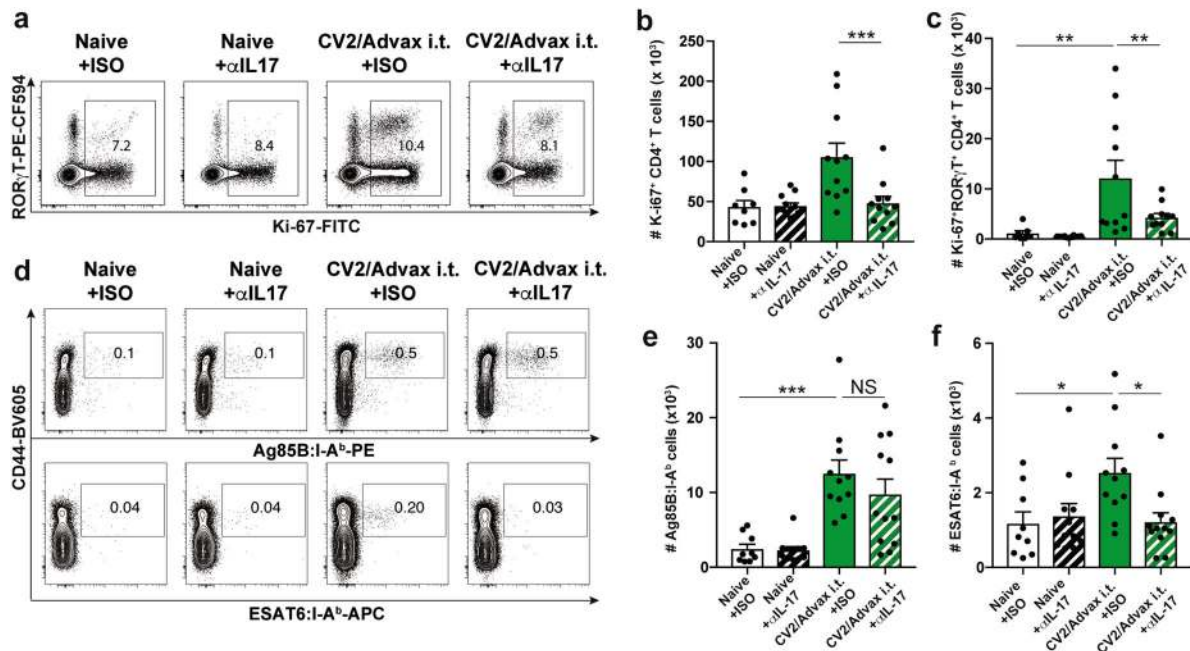


**Fig. 7** Blocking IL-17 during *M. tuberculosis* infection impairs the proliferation of pathogen-specific CD4<sup>+</sup> T cells in the mediastinal lymph nodes. C57BL/6 mice ( $n = 5-6$ ) were vaccinated with CysVac2/Advax and treated i.p. with anti-IL-17 mAb, as described in Fig. 5. Representative dot plot of the expression of Ki67 and ROR $\gamma$ T on CD4<sup>+</sup> T cells (a). Bar graphs show the average numbers of the total (b) and ROR $\gamma$ T<sup>+</sup> (c) proliferating CD4<sup>+</sup> T cells enumerated in the mLN  $\pm$  SEM. Representative dot plots show CD44 and either Ag85B:I-A<sup>b</sup> or ESAT6:I-A<sup>b</sup> staining on CD4<sup>+</sup> T cells in the mLN (d), with total number  $\pm$  SEM of Ag85B:I-A<sup>b</sup> (e), and ESAT6:I-A<sup>b</sup> (f) CD4<sup>+</sup> T cells in the mLN. Data are pooled from two independent experiments. The significance of differences between the groups was determined by ANOVA (\* $p < 0.05$ ; \*\* $p < 0.01$ ; \*\*\* $p < 0.001$ ).

## DISCUSSION

The respiratory tract is the preferred port of entry of *M. tuberculosis*, with the complexity of the immunological environment in the lung potentially contributing to suboptimal pathogen responses. This may be particularly detrimental in the case of *M. tuberculosis* infection, where priming and recruitment of effector T lymphocytes to the lungs is delayed, allowing unchecked growth of the organism<sup>24,25</sup>. For this reason, mucosal vaccination has been of interest in the field of TB vaccines, with pulmonary delivery of BCG<sup>14,26</sup>, live recombinant viruses<sup>8,27,28</sup>, or protein/adjuvants<sup>29,30</sup> resulting in protective immune responses. When administered to the respiratory mucosa, highly inflammatory adjuvanted vaccines may induce protective immunity, but this is often accompanied by excessive inflammation, mucus accumulation, and eosinophilia<sup>31</sup>. Thus, there is a need for adjuvants that can induce protective lung immunity in the absence of deleterious inflammation and pathology. We found that i.t. delivery of CysVac2/Advax<sup>CPG</sup> was significantly more protective than i.m. vaccination against challenge with *M. tuberculosis* (Fig. 1). Strikingly, i.t. vaccination, despite being more protective, did not induce appreciable numbers of multifunctional CD4<sup>+</sup> T cells (IFN- $\gamma$ <sup>+</sup>IL-2<sup>+</sup>TNF<sup>+</sup>; Fig. 1) and even more surprisingly removal of CpG from the formulation did not reduce vaccine protection, despite a loss of multifunctional CD4<sup>+</sup> T cell generation (Fig. 2). Induction of multifunctional T cell responses has been used as a key criterion for vaccine progression to human trials, however recent evidence in both mice and humans indicates that the generation of IFN- $\gamma$  secreting T cells does not necessarily correlate with protection<sup>32</sup>. Indeed, in our data IFN- $\gamma$  was the only cytokine analyzed pre- and post-challenge that did not correlate with the protective effect of the CysVac2/Advax vaccine (Fig. 5), an important finding for the selection of vaccines for progression to human trials.

We observed that pulmonary vaccination with CysVac2 vaccination induced a lung-resident CD4<sup>+</sup> population that expressed markers of T<sub>RM</sub>-like cells (Fig. 4). We have previously shown that a

recombinant influenza vaccine conferred protection against *M. tuberculosis* in the absence of circulating memory T cells, suggesting an important role for *M. tuberculosis*-specific T<sub>RM</sub><sup>8</sup>. In the current study, detailed phenotypic analysis of CysVac2/Advax-induced, antigen-specific CD4<sup>+</sup> T<sub>RM</sub>-like cells showed that in addition to well-characterized markers of tissue-resident memory cells (CD69<sup>+</sup>CD44<sup>hi</sup>CD62L<sup>low</sup>CD45<sup>IV</sup>-), this population displayed high levels of CD11a with minimal expression of CD103 (Fig. 4). This low level of CD103 expression contrasts with the increased expression of CD103 on CD8<sup>+</sup> T<sub>RM</sub>, where this integrin is thought to be essential in the retention of these cells within tissue<sup>33</sup>. We also noted the distinct formation of iBalt structures in the lung after CysVac2/Advax-delivery (Fig. 3); iBalt is thought to provide a survival niche for T<sub>RM</sub> and thus may participate in the protective response afforded by CysVac2/Advax vaccination<sup>34</sup>. Antigen-specific T<sub>RM</sub> cells induced following CysVac2/Advax vaccination also displayed a dominant PD-1<sup>+</sup>KLRG-1<sup>-</sup> phenotype (Fig. 4). During *M. tuberculosis* infection, PD-1 expression indicates an earlier stage of CD4<sup>+</sup> T cell differentiation that is associated with a higher proliferative capacity, while KLRG-1<sup>+</sup> cells are more terminally differentiated and produce greater levels of cytokines<sup>35</sup>. IL-2-secreting KLRG-1<sup>-</sup> T cells induced by subunit booster vaccination are associated with protection against chronic *M. tuberculosis*, owing to the maintenance of their proliferative capacity<sup>36</sup>, and circulating KLRG-1<sup>-</sup> CD4<sup>+</sup> T cells induced by subcutaneous H56/CAF01 vaccination display the ability to home to the lungs<sup>37</sup>. Our findings confirmed an association between vaccine-induced, PD-1<sup>+</sup>KLRG-1<sup>-</sup> CD4<sup>+</sup> T cells that reside within the lung parenchyma and protection against *M. tuberculosis*. It is possible these cells possess greater effector functions and proliferative capacity than their KLRG-1<sup>+</sup> counterparts and are therefore capable of enhanced protection against *M. tuberculosis* infection.

Lung-resident CD4<sup>+</sup> T<sub>RM</sub> was found to be an important source of IL-17 induced after Advax:CysVac2 i.t. delivery, and this was not observed after i.m. delivery of the vaccine. This is in agreement

with other studies showing that IL-17 is strongly induced following mucosal vaccination and correlates with protection against *M. tuberculosis* infection<sup>38,39</sup>, yet the mechanism by which this protection is specifically mediated is not well defined. Blocking of IL-17 during *M. tuberculosis* challenge in CysVac2/Advax-vaccinated mice resulted in a complete loss of vaccine-induced protection and correlated with reduced recruitment of lung phagocytic cells such as neutrophils and macrophages, as well as reduced priming of *M. tuberculosis*-specific T cells in the mLN (Figs. 6 and 7). Thus we can propose a mechanism whereby IL-17 production by vaccine-specific CD4<sup>+</sup> T<sub>RM</sub> facilitates neutrophil and monocyte/macrophage recruitment<sup>11</sup>, and promotes the activation and proliferation of protective, pathogen-specific CD4<sup>+</sup> T cells in the mLN<sup>40–42</sup>. Interstitial macrophages recruitment might be beneficial because these populations appear to possess significant antimycobacterial activity, as opposed to alveolar macrophages<sup>43</sup>. Previous work in a different infectious model has additionally demonstrated that IL-17 can mediate the recruitment of neutrophils with anti-bacterial potential<sup>11</sup>. Our observations differ from previous reports using the ID93 + GLA-SE mucosal TB vaccine, which resulted in a Th17-dominated, tissue-resident response but did not lead to improved protection when compared to parenteral immunization<sup>44</sup>. This may indicate that different adjuvants may induce diverse T<sub>RM</sub> populations, and the capacity of Advax to direct a predominant, vaccine-specific T<sub>RM</sub> response in the lung may be a key determinant in the protective efficacy of CysVac2/Advax vaccine.

Harnessing the protective role of IL-17 against pathogens needs to be balanced with potential tissue damage and pathology associated with excess cytokine levels<sup>15</sup>. Thus, adjuvants stimulating excessive levels of IL-17 are unlikely to be suitable for human lung administration, as observed for a candidate Sporotrichosis vaccine<sup>45</sup>. When CpG was removed from the CysVac2/Advax vaccine, the frequency of IL-17 secreting T cells in the lung was reduced, yet protection against *M. tuberculosis* challenge was not affected (Fig. 2 and Supplementary Fig. 3). This suggests that a threshold of IL-17-secreting T cells may exist for vaccine-induced protection against *M. tuberculosis* and selecting the most “immunogenic” vaccines based on the greatest level of effector responses may not be the best strategy for identifying an optimal *M. tuberculosis* vaccine formulation.

In conclusion, this report demonstrates that Advax-adjuvanted vaccines can be safely delivered to the lung to provide significant protection against aerosol *M. tuberculosis* infection. The protective effect of the vaccine was associated with the targeted expansion of lung-resident T<sub>RM</sub> and was dependent on IL-17 recruitment of phagocytic cells to the lung and enhanced priming of T cells in the mLN. Advax-containing vaccines have proven safe and immunogenic in human trials against viral infection and allergy<sup>19,46,47</sup> and are safe and effective in pre-clinical trials as inhaled formulations<sup>21</sup>. Thus CysVac2/Advax warrants further study to assess its suitability as a pulmonary vaccine for the control of TB in humans.

## METHODS

### Ethics statement

Female C57BL/6 (6–8 weeks of age) were purchased from Australian BioResources (NSW, Australia), and housed at the Centenary Institute animal facility (Sydney, Australia) in specific pathogen-free conditions. All mouse work was performed according to ethical guidelines as set out by the Sydney Local Health District (SLHD) Animal Ethics and Welfare Committee, which adhere to the Australian Code for the Care and Use of Animals for Scientific Purposes (2013) as set out by the National Health and Medical Research Council of Australia. All experiments within this manuscript were approved under protocol number 2017/011 by the SLHD Animal Ethics and Welfare Committee.

### Bacterial strains

*M. tuberculosis* H37Rv (BEI Resources, USA) and BCG Pasteur were grown at 37 °C in Middlebrook 7H9 medium (Becton Dickinson, BD) supplemented with 0.5% glycerol, 0.02% Tyloxapol, and 10% albumin-dextrose-catalase (ADC), or on solid Middlebrook 7H11 medium (BD) supplemented with oleic acid–ADC.

### Mouse immunization, treatments, and infection

CysVac2 fusion protein (Ag85B-CysD) was recombinantly expressed in *E. coli*, purified from inclusions bodies by ChinaPeptides (Shanghai, China), and refolded in Tris-buffer. Advax (delta-inulin, 50 mg/ml) and Advax<sup>CpG</sup> (delta-inulin plus CpG, 50 mg/ml and 500 µg/ml, respectively) were provided by Vaxine Pty Ltd (Adelaide, Australia). Mice were anesthetized by intraperitoneal (i.p.) injection of Ketamine/Xylazine (80/100 mg/kg mouse) and then vaccinated with 1 mg of Advax or Advax<sup>CpG</sup> and 3 µg of CysVac2 in a final volume of 50 µl PBS via i.m. route, using an insulin syringe (BD), or via the i.t. route, using PennCentury Microsprayer Aerosoliser (PennCentury, PA, USA). Three µg of CysVac2 alone or sterile PBS were administered as controls where appropriate. Mice were immunized subcutaneously with 5 × 10<sup>5</sup> BCG for protection experiments.

For neutralization of IL-17, mice were injected i.p. with 250 µg of anti-IL-17A (clone TC11-18H10.1, Biologend) or isotype control (clone RTK2071, Biologend) one day prior to *M. tuberculosis* infection and then every three days for three weeks.

For *M. tuberculosis* challenge experiments, 6 or 8 weeks after the last vaccination mice were infected with *M. tuberculosis* H37Rv via the aerosol route using a Middlebrook airborne infection apparatus (Glas-Col, IN, USA) with an infective dose of ~100 viable bacilli. Three or 4 weeks later, the lungs and spleen were harvested, homogenized, and plated after serial dilution on supplemented Middlebrook 7H11 agar plates. Colonies forming units (CFU) were determined 3 weeks later and expressed as log<sub>10</sub> CFU.

For intravascular staining of leucocytes, 3 min before euthanasia, mice were i.v. injected with 200 µl biotin-conjugated anti-CD45 mAb in PBS (15 µg/ml, Biologend, clone 104) into the lateral tail vein. The detection of biotin was performed with APC-Cy7-conjugated streptavidin (BioLegend).

### Cell isolation, peptide stimulations, and flow cytometry

Mice were bled from the lateral tail vein and the PBMCs were isolated from whole blood by stratifying unclotted whole blood on Histopaque1083 (Sigma-Aldrich). Single-cell suspensions were prepared from the lung by digesting the tissue with Collagenase IV and DNase (Sigma-Aldrich) for 45 min and dissociated using a gentleMACS dissociator (Miltenyi Biotec), the cell recovered were incubated in ACK lysis buffer to remove red blood cells. PE-conjugated Ag85B<sub>240–254</sub>:I-A<sup>b</sup> tetramer and APC-conjugated ESAT6<sub>1–20</sub>:I-A<sup>b</sup> tetramer were provided by the NIH Tetramer Core Facility. For staining, cells were incubated with tetramers at a 1:200 dilution for 1 h at 37 °C. Cells were stained using the marker-specific fluorochrome-labeled mAbs indicated in Supplementary Table 1. The gating strategy for the identification of specific cell populations is shown in Supplementary Fig. 1. To assess antigen-specific cytokine induction by T cells, PBMCs or single-cell suspensions from the lung were stimulated for 4 h with CysVac2 (5 µg/ml) and then supplemented with brefeldin A (10 µg/ml) for a further 10–12 h. Cells were surface stained with Fixable Blue Dead Cell Stain (Life Technologies) and the marker-specific fluorochrome-labeled antibodies indicated in Supplementary Table. Cells were then fixed and permeabilized using the BD Cytotfix/Cytoperm<sup>TM</sup> kit according to the manufacturer's protocol. When required, intracellular staining was performed using mAbs against the specific cytokines (Supplementary Table 1). Samples were acquired on a BD LSR-Fortessa (BD) and analyzed using FlowJo<sup>TM</sup> analysis software (Treestar, USA). A Boolean combination of gates was used to calculate the frequency of single-, double- and triple-positive CD4<sup>+</sup> T cell subsets. tSNE was run using default FlowJo parameters (iterations = 1000, perplexity = 30). Samples were randomly downsampled to 2000 events per sample and analysis was run on equal numbers of events per sample using the FlowJo tSNE plugin.

### Detection of anti-CysVac2 antibodies

Microtiter plates were incubated overnight with 5 µg/ml CysVac2 antigen at 4 °C, blocked with 3% BSA, and serially diluted serum samples were incubated for 1 h at RT. Plates were washed and biotinylated polyclonal goat anti-mouse IgG2c (1:10,000, Abcam, cat# ab97253), rat anti-mouse IgG1 (1:500, clone RMG1-1, Biologend, cat# 406603) or rat anti-mouse IgA

(1:250, clone RMA-1, Biolegend, cat# 407003) added for 1 h at RT. After incubation with streptavidin-HRP (1:1,000, BioLegend, cat# 405210) for 30 min at RT, binding was visualized by the addition of tetramethyl benzene (Sigma-Aldrich). The reaction was stopped with the addition of H<sub>2</sub>SO<sub>4</sub> and absorbances were measured at 450 nm. Titers were calculated with GraphPad Prism 6 software (GraphPad Software, USA) as the dilution of the sample that reaches the average of the control serum  $\pm$  3 standard deviations.

### Immunofluorescence staining

Following perfusion, the superior right lung lobe from euthanized mice was excised and inflated with 4% paraformaldehyde (ThermoScientific) in PBS using a needle and syringe. Following fixation, lobes were transferred to 20% sucrose solution and then snap frozen at  $-80^{\circ}\text{C}$  in Optimal Cutting Temperature compound (VWR chemicals). Lobes were sectioned using a Cytotome E (ThermoScientific) to 12  $\mu\text{m}$  thickness and slide allowed to dry at RT overnight before storage at  $-80^{\circ}\text{C}$ . Prior to staining, slides were washed in PBS and non-specific antibody binding blocked with 3% Normal Goat Serum (Sigma) with 0.1% Triton-X 100 (Sigma) in PBS. Slides were probed with AF488-conjugated anti-mouse-CD3 at 1:100 dilution (Clone 17A2, Biolegend, cat# 100210) and AF594-conjugated anti-mouse-B200 at 1:200 dilution (Clone RA3-6B2, Biolegend, cat# 103254) to visualize T and B cells, and NucBlue fixed cell stain ReadyProbes reagent (Life Technologies) to stain nuclei. Following staining, samples were mounted with Prolong Diamond Antifade mountant (Thermo Fisher) and imaged using a BX51 microscope (Olympus, Japan) microscope.

### Statistical analysis

Statistical analysis was performed using GraphPad Prism 6 software (GraphPad Software, USA). The significance of differences between experimental groups was evaluated by one-way analysis of variance (ANOVA), with a pairwise comparison of multi-grouped data sets achieved using the Tukey post-hoc test. Differences are considered as statistically different when  $p \leq 0.01$ .

### Reporting summary

Further information on research design is available in the Nature Research Reporting Summary linked to this article.

### DATA AVAILABILITY

The authors confirm that all relevant data are included in the paper and its Supplementary Information.

Received: 11 March 2020; Accepted: 2 October 2020;

Published online: 12 November 2020

### REFERENCES

- World Health Organisation. *Global Tuberculosis Report 2019* (WHO, 2019).
- Mangtani, P. et al. Protection by BCG vaccine against tuberculosis: a systematic review of randomized controlled trials. *Clin. Infect. Dis.* **58**, 470–480 (2014).
- Knight, G. M. et al. Impact and cost-effectiveness of new tuberculosis vaccines in low- and middle-income countries. *Proc. Natl Acad. Sci. USA* **111**, 15520–15525 (2014).
- Kaufmann, S. H., Weiner, J. & von Reyn, C. F. Novel approaches to tuberculosis vaccine development. *Int J. Infect. Dis.* **56**, 263–267 (2017).
- Van Der Meeren, O. et al. Phase 2b controlled trial of M72/AS01E vaccine to prevent tuberculosis. *N. Engl. J. Med.* **379**, 1621–1634 (2018).
- Tait, D. R. et al. Final analysis of a trial of M72/AS01E vaccine to prevent tuberculosis. *N. Engl. J. Med.* **381**, 2429–2439 (2019).
- Shim, B. S. et al. Development of safe and non-self-immunogenic mucosal adjuvant by recombinant fusion of cholera toxin A1 subunit with protein transduction domain. *J. Immunol. Res.* **2018**, 9830701 (2018).
- Florido, M. et al. Pulmonary immunization with a recombinant influenza A virus vaccine induces lung-resident CD4<sup>(+)</sup> memory T cells that are associated with protection against tuberculosis. *Mucosal Immunol.* **11**, 1743–1752 (2018).
- Darrah, P. A. et al. Prevention of tuberculosis in macaques after intravenous BCG immunization. *Nature* **577**, 95–102 (2020).
- Perdomo, C. et al. Mucosal BCG vaccination induces protective lung-resident memory T cell populations against tuberculosis. *MBio* **7**, e01686-16 (2016).
- Flannigan, K. L. et al. IL-17A-mediated neutrophil recruitment limits expansion of segmented filamentous bacteria. *Mucosal Immunol.* **10**, 673–684 (2017).
- Khader, S. A. et al. IL-23 and IL-17 in the establishment of protective pulmonary CD4<sup>(+)</sup> T cell responses after vaccination and during *Mycobacterium tuberculosis* challenge. *Nat. Immunol.* **8**, 369–377 (2007).
- Ahmed, M. et al. A novel nanoemulsion vaccine induces mucosal Interleukin-17 responses and confers protection upon *Mycobacterium tuberculosis* challenge in mice. *Vaccine* **35**, 4983–4989 (2017).
- Moliva, J. I. et al. Selective delipidation of *Mycobacterium bovis* BCG enables direct pulmonary vaccination and enhances protection against *Mycobacterium tuberculosis*. *Mucosal Immunol.* **12**, 805–815 (2019).
- Das, S. & Khader, S. Yin and yang of interleukin-17 in host immunity to infection. *F1000Res* **6**, 741 (2017).
- Counoupas, C. et al. Delta inulin-based adjuvants promote the generation of polyfunctional CD4<sup>(+)</sup> T cell responses and protection against *Mycobacterium tuberculosis* infection. *Sci. Rep.* **7**, 8582 (2017).
- Counoupas, C. et al. *Mycobacterium tuberculosis* components expressed during chronic infection of the lung contribute to long-term control of pulmonary tuberculosis in mice. *NPJ Vaccines* **1**, 16012 (2016).
- Feinen, B., Petrovsky, N., Verma, A. & Merkel, T. J. Advax-adjuvanted recombinant protective antigen provides protection against inhalational anthrax that is further enhanced by addition of murabutide adjuvant. *Clin. Vaccin. Immunol.* **21**, 580–586 (2014).
- Gordon, D. L. et al. Human Phase 1 trial of low-dose inactivated seasonal influenza vaccine formulated with Advax delta inulin adjuvant. *Vaccine* **34**, 3780–3786 (2016).
- Tomar, J. et al. Passive inhalation of dry powder influenza vaccine formulations completely protects chickens against H5N1 lethal viral challenge. *Eur. J. Pharm. Biopharm.* **133**, 85–95 (2018).
- Tomar, J. et al. Advax augments B and T cell responses upon influenza vaccination via the respiratory tract and enables complete protection of mice against lethal influenza virus challenge. *J. Control Release* **288**, 199–211 (2018).
- Chu, R. S., Targoni, O. S., Krieg, A. M., Lehmann, P. V. & Harding, C. V. CpG oligodeoxynucleotides act as adjuvants that switch on T helper 1 (Th1) immunity. *J. Exp. Med.* **186**, 1623–1631 (1997).
- Park, C. O. & Kupper, T. S. The emerging role of resident memory T cells in protective immunity and inflammatory disease. *Nat. Med.* **21**, 688–697 (2015).
- Reiley, W. W. et al. ESAT-6-specific CD4 T cell responses to aerosol *Mycobacterium tuberculosis* infection are initiated in the mediastinal lymph nodes. *Proc. Natl Acad. Sci. USA* **105**, 10961–10966 (2008).
- Wolf, A. J. et al. Initiation of the adaptive immune response to *Mycobacterium tuberculosis* depends on antigen production in the local lymph node, not the lungs. *J. Exp. Med.* **205**, 105–115 (2008).
- Bull, N. C. et al. Enhanced protection conferred by mucosal BCG vaccination associates with presence of antigen-specific lung tissue-resident PD-1<sup>(+)</sup> KLRG1<sup>(-)</sup> CD4<sup>(+)</sup> T cells. *Mucosal Immunol.* **12**, 555–564 (2019).
- Green, C. A. et al. Novel genetically-modified chimpanzee adenovirus and MVA-vectored respiratory syncytial virus vaccine safely boosts humoral and cellular immunity in healthy older adults. *J. Infect.* **78**, 382–392 (2019).
- Manjaly Thomas, Z. R. et al. Alternate aerosol and systemic immunisation with a recombinant viral vector for tuberculosis, MVA85A: a phase I randomised controlled trial. *PLoS Med.* **16**, e1002790 (2019).
- Van Dis, E. et al. STING-activating adjuvants elicit a Th17 immune response and protect against *Mycobacterium tuberculosis* infection. *Cell Rep.* **23**, 1435–1447 (2018).
- Copland, A. et al. Mucosal delivery of fusion proteins with *Bacillus subtilis* spores enhances protection against tuberculosis by Bacillus Calmette-Guérin. *Front. Immunol.* **9**, 346 (2018).
- Kim, K. H. et al. Alum adjuvant enhances protection against respiratory syncytial virus but exacerbates pulmonary inflammation by modulating multiple innate and adaptive immune cells. *PLoS ONE* **10**, e0139916 (2015).
- Rodo, M. J. et al. A comparison of antigen-specific T cell responses induced by six novel tuberculosis vaccine candidates. *PLoS Pathog.* **15**, e1007643 (2019).
- Wakim, L. M., Woodward-Davis, A. & Bevan, M. J. Memory T cells persisting within the brain after local infection show functional adaptations to their tissue of residence. *Proc. Natl Acad. Sci. USA* **107**, 17872–17879 (2010).
- Schreiner, D. & King, C. G. CD4<sup>(+)</sup> memory T cells at home in the tissue: mechanisms for health and disease. *Front. Immunol.* **9**, 2394 (2018).
- Reiley, W. W. et al. Distinct functions of antigen-specific CD4 T cells during murine *Mycobacterium tuberculosis* infection. *Proc. Natl Acad. Sci. USA* **107**, 19408–19413 (2010).



36. Lindstrom, T., Knudsen, N. P., Agger, E. M. & Andersen, P. Control of chronic mycobacterium tuberculosis infection by CD4 KLRG1- IL-2-secreting central memory cells. *J. Immunol.* **190**, 6311–6319 (2013).
37. Woodworth, J. S. et al. Subunit vaccine H56/CAF01 induces a population of circulating CD4 T cells that traffic into the *Mycobacterium tuberculosis*-infected lung. *Mucosal Immunol.* **10**, 555–564 (2017).
38. Aguilo, N. et al. Pulmonary but not subcutaneous delivery of BCG vaccine confers protection to tuberculosis-susceptible mice by an interleukin 17-dependent mechanism. *J. Infect. Dis.* **213**, 831–839 (2016).
39. Gopal, R. et al. Interleukin-17-dependent CXCL13 mediates mucosal vaccine-induced immunity against tuberculosis. *Mucosal Immunol.* **6**, 972–984 (2013).
40. Liang, F. et al. Vaccine priming is restricted to draining lymph nodes and controlled by adjuvant-mediated antigen uptake. *Sci. Transl. Med.* **9**, eaal2094 (2017).
41. Morel, C. et al. Mycobacterium bovis BCG-infected neutrophils and dendritic cells cooperate to induce specific T cell responses in humans and mice. *Eur. J. Immunol.* **38**, 437–447 (2008).
42. Blomgran, R. & Ernst, J. D. Lung neutrophils facilitate activation of naive antigen-specific CD4<sup>+</sup> T cells during *Mycobacterium tuberculosis* infection. *J. Immunol.* **186**, 7110–7119 (2011).
43. Huang, L., Nazarova, E. V., Tan, S., Liu, Y. & Russell, D. G. Growth of Mycobacterium tuberculosis in vivo segregates with host macrophage metabolism and ontogeny. *J. Exp. Med.* **215**, 1135–1152 (2018).
44. Orr, M. T. et al. Mucosal delivery switches the response to an adjuvanted tuberculosis vaccine from systemic TH1 to tissue-resident TH17 responses without impacting the protective efficacy. *Vaccine* **33**, 6570–6578 (2015).
45. Portuondo, D. L. et al. Comparative efficacy and toxicity of two vaccine candidates against *Sporothrix schenckii* using either Montanide Pet Gel A or aluminum hydroxide adjuvants in mice. *Vaccine* **35**, 4430–4436 (2017).
46. Gordon, D., Kelley, P., Heinzel, S., Cooper, P. & Petrovsky, N. Immunogenicity and safety of Advax, a novel polysaccharide adjuvant based on delta inulin, when formulated with hepatitis B surface antigen: a randomized controlled Phase 1 study. *Vaccine* **32**, 6469–6477 (2014).
47. Heddle, R., Smith, A., Woodman, R., Hissaria, P. & Petrovsky, N. Randomized controlled trial demonstrating the benefits of delta inulin adjuvanted immunotherapy in patients with bee venom allergy. *J. Allergy Clin. Immunol.* **144**, 504–513.e516 (2019).

## ACKNOWLEDGEMENTS

This work was supported by a National Health and Medical Research Council (NHMRC) Project Grant (APP1043519), the NHMRC Centre of Research Excellence in Tuberculosis Control (APP1043225), and the Australian Respiratory Council Windsor grant scheme. We acknowledge the support of the European H2020 grant TBVAC2020 15 643381, the provision of reagents through the NIH Tetramer Core Facility, and assistance from the Advanced Cytometry Facility and animal facility at the Centenary Institute. N.P. is supported by the National Institutes of Health contract

HHSN272201400053C and the development of the Advax adjuvant was supported by NIH Contracts AI061142 and HHSN272200800039C.

## AUTHOR CONTRIBUTIONS

C.C., N.P., W.J.B., and J.A.T. conceived and designed the study. C.C., A.A., K.F., G.N., E.S., and N.D.B. performed the experiments. All authors processed and analyzed the data. C.C. and J.A.T. wrote the first draft of the manuscript, all authors reviewed and approved the final manuscript version.

## COMPETING INTERESTS

N.P. is the research director for Vaxine P/L. E.L.S. was an employee of Vaxine P/L. The remaining authors declare that they have no competing interests.

## ADDITIONAL INFORMATION

**Supplementary information** is available for this paper at <https://doi.org/10.1038/s41541-020-00255-7>.

**Correspondence** and requests for materials should be addressed to C.C. or J.A.T.

**Reprints and permission information** is available at <http://www.nature.com/reprints>

**Publisher's note** Springer Nature remains neutral with regard to jurisdictional claims in published maps and institutional affiliations.



**Open Access** This article is licensed under a Creative Commons Attribution 4.0 International License, which permits use, sharing, adaptation, distribution and reproduction in any medium or format, as long as you give appropriate credit to the original author(s) and the source, provide a link to the Creative Commons license, and indicate if changes were made. The images or other third party material in this article are included in the article's Creative Commons license, unless indicated otherwise in a credit line to the material. If material is not included in the article's Creative Commons license and your intended use is not permitted by statutory regulation or exceeds the permitted use, you will need to obtain permission directly from the copyright holder. To view a copy of this license, visit <http://creativecommons.org/licenses/by/4.0/>.

© Crown 2020